

T.A. GAVRILKO,¹ G.O. PUCHKOVSKA,¹ V.I. STYOPKIN,¹ T.V. BEZRODNA,¹
J. BARAN,² M. DROZD²

¹Institute of Physics, Nat. Acad. of Sci. of Ukraine
(46, Prosp. Nauky, Kyiv 03028, Ukraine; e-mail: gavrilko@iop.kiev.ua)

²Institute of Low Temperatures and Structure Research, PAN
(2, Okolna Str., Wroclaw, Poland)

MOLECULAR DYNAMICS AND PHASE TRANSITIONS BEHAVIOR OF BINARY MIXTURES OF FATTY ACIDS AND CETYLTRIMETHYLAMMONIUM BROMIDE AS STUDIED VIA DAVYDOV SPLITTING OF MOLECULAR VIBRATIONAL MODES

PACS 43.20Tb, 71.70.-d,
81.30.Dz

The 1:1 solid phase complexes of stearic (SA) and behenic (BA) fatty acids (FA) with cationic surfactant cetyltrimethylammonium bromide (CTAB) are prepared from an equimolar ethanol solution of their binary mixtures. A supramolecular complexation between FA and CTAB molecules is proven with FTIR spectroscopy, X-ray diffraction (XRD), and differential scanning calorimetry (DSC). A single-phase layered crystalline structure of both CTAB:SA and CTAB:BA complexes is revealed by XRD. The greatly enhanced thermal stability of the CTAB:FA complexes over the pure FA (by about 40–50° C) is found with DSC along with a number of successive solid-solid phase transitions. The temperature-dependent FTIR study of the Davydov splitting for CH₂ rocking (720–730 cm⁻¹) vibrations revealed a significant difference in the conformational disorder of methylene chains and the molecular packing in successive solid phases of CTAB:SA and CTAB:BA complexes. Our research provides a molecular basis for a prospective application of such class of binary mixtures of oppositely charged cationic and anionic surfactants in thermo-sensitive supramolecular systems.

Keywords: FTIR spectroscopy, X-ray diffraction, DSC, CTAB, fatty acids, supramolecular complex.

1. Introduction

Binary mixtures of oppositely charged cationic and anionic surfactants, the so-called catanionic surfactants (CAS), are attracting a lot of interest during the past decades due to their remarkable ability to form a variety of self-assembled structures both on a solid surface and in an air-water interface [1–8]. These structures range from micelles to

bilayers, nanotubes, and vesicles, and are of a great application potential in nanotechnology for the synthesis of various nanoobjects, as well as for various encapsulation and controlled-delivery processes in pharmacy, medicine, and biology. Though the behavior of CAS was most intensively studied in water solutions, it was recently shown that equimolar mixtures of cationic and anionic surfactants exhibit a rich polymorphism in the condensed state [9–12], both in the bulk or self-assembled monolayer. It was found that the phase transition pattern in such complexes depends on many factors, among them the na-

© T.A. GAVRILKO, G.O. PUCHKOVSKA,
V.I. STYOPKIN, T.V. BEZRODNA, J. BARAN,
M. DROZD, 2013

ture of cationic and anionic head groups, a relationship between the alkyl chain lengths, relative concentration of components, *etc.* [13, 14]. However, the solid state properties of these systems are still far from being fairly understood and, therefore, require a comprehensive study. It should be mentioned that lipid bilayers and vesicle shells comprise the CAS in a solid phase, which determines, to a large extent, their thermal stability and permeability. Therefore, there is a need to investigate the solid-state CAS structure, thermal properties, and phase behavior in more details. For this reason, we report on the comprehensive study of 1:1 solid phase complexes of a cationic surfactant cetyltrimethylammonium bromide (CTAB), $[\text{H}_3\text{C}(\text{CH}_2)_{15}\text{N}^+(\text{CH}_3)_3]^+\text{Br}^-$, with a fatty acid (FA) as an anionic surfactant. Two FAs were used: stearic ($\text{H}_3\text{C}(\text{CH}_2)_{16}\text{COOH}$, SA) and behenic ($\text{H}_3\text{C}(\text{CH}_2)_{20}\text{COOH}$, BA) acids. Our particular interest was focused on the complexation nature, in which the interaction between the acid surfactant and the CTA^+ counterion plays the leading role, and its effect on the thermal stability of the FA:CTAB complexes. The molecular packing and the hydrocarbon chain conformational order in various solid phases of the complexes were investigated with regard for the possible molecular mechanisms of successive phase transitions.

2. Experimental

The initial compounds, CTAB (Fluka, 99%), SA and BA fatty acids (Sigma-Aldrich) were used without any treatment. The CTAB:SA and CTAB:BA complexes were prepared from an equimolar ethanol solution of corresponding binary mixtures. First, polycrystalline FA was dissolved in bi-distilled ethanol heated up to 55–60°C. The FA concentration in the ethanol solution was about 3% wt. Then the equimolar quantity of CTAB was added to the solution. The resulting solution was kept at an elevated temperature for half an hour to ensure the reaction between the components takes place. Then ethanol was left to fully evaporate, and the resulting complexes CTAB:SA or CTAB:BA were obtained as a solid white precipitate.

The crystal structure of the CTAB:SA and CTAB:BA complexes, as well as their pure components CTAB, SA, and BA, was studied by X-ray powder diffraction. The XRD patterns were obtained

at room temperature with a 139 DRON-3M X-ray diffractometer. $\text{CuK}\alpha$ radiation filtered with a Ni foil was used for these experiments.

The thermotropic properties of the CTAB:SA and CTAB:BA complexes were measured in the temperature interval 20–130 °C with a Perkin–Elmer DSC7 differential scanning calorimeter for a sample weight of 3.5–6 mg at a scanning rate of 8 °C/min. A standard indium sample served for a calibration of the enthalpy values. For comparison, DSC curves for initial compounds (CTAB, SA, and BA) were measured. The phase transition parameters, transition temperatures, and changes in the enthalpy were derived from DSC data on heating and cooling cycles.

Temperature-variable FTIR transmission spectra of the investigated CTAB:SA and CTAB:BA complexes pressed in KBr pellets, as well as initial compounds CTAB, SA and BA, were measured with a Bruker IFS-88 FTIR spectrometer in the 400–4000 cm^{-1} spectral range. The spectral resolution was 1 and 4 cm^{-1} , and 128 scans were accumulated for each spectrum. The spectra were measured in the 20–130 °C temperature interval that corresponds to the conditions for the DSC curves recording. A SPECAC variable temperature cell P/N 21.500 and an automatic temperature controller P/N 20120 series equipped with an Eurotherm 847 controller were used for these measurements.

3. Results and Discussions

3.1. X-ray diffraction studies

X-ray diffraction studies show that, similarly to the initial CTAB, SA, and BA compounds, both CTAB:SA and CTAB:BA complexes do crystallize in such a way that their molecules are arranged in a layered structure. XRD patterns of the investigated compounds are shown in Fig. 1. From Fig. 1, *a*, it can be seen that the diffraction maxima from CTAB:BA are located very close to those from crystalline BA. The diffraction reflections related to crystalline CTAB are also close to these positions, though slightly displaced. This observation proves that the molecular packing in the CTAB:BA solid phase is similar to that of the initial compounds. The calculated basic bilayer distance of CTAB:BA complex ($d = 5.49$ nm) is also close to that of pure components BA ($d = 5.53$ nm) and CTAB ($d = 5.25$ nm). Assuming a structure of the complex as a bi-tailed molecule

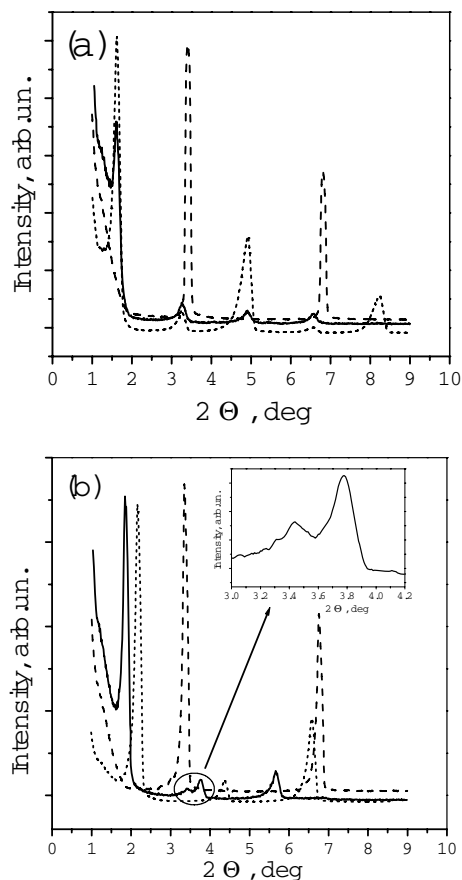


Fig. 1. X-ray diffraction patterns for: CTAB:BA (solid), BA (short dashed) and CTAB (dashed) (a) and CTAB:SA (solid), SA (short dashed) and CTAB (dashed) (b). The inset shows the enlarged part of the XRD pattern

with a central head-group in the middle, the length of the new CTAB:BA molecule can be estimated as being 5.84 nm. Using this value, the tilt of CTAB:BA molecules to the layer plane was calculated and appeared to be 67° . This value is close to the molecular tilt angles of the initial CTAB and BA, whose calculated values are equal to 65° and 66° , correspondingly.

Contrary to CTAB:BA, the diffraction pattern of CTAB:SA is significantly different, as compared with those of initial CTAB and SA (Fig. 1, b). From the inset in Fig. 1, b showing the enlarged part of the XRD pattern of CTAB:SA, two weaker diffraction peaks can be observed at 3.43° and 3.78° . At the same time, the XRD pattern of CTAB:BA shows only one peak in this angular range centered at 3.26° . Neither of these two peaks coincides with the diffraction maxima of

the initial compounds. So they could be attributed to the X-ray diffraction from CTAB:SA complex, and not from the remnants of the initial compounds. To evaluate the molecular orientation in the CTAB:SA solid phase, we assumed that the diffraction peak centered at 3.43° corresponds to the CTAB-related part of the molecular complex, while that at 3.78° corresponds to its SA-related part. Starting from the lengths of 2.87 nm for CTAB and 2.5 nm for an SA molecule, we calculated the tilt of the SA-related molecular tail, as being equal to 66° , and that of the CTAB-related molecular part as 61° . These values are different from the molecular tilt angles found for the room-temperature solid phase of pure CTAB (65°) and SA (53°). It is clear that a variation in the tilt angle means the changes both in the head-group arrangement and the alkyl chain packing in these two complexes [10, 11].

Our XRD results show that the alkyl chains in solid CTAB:SA and CTAB:BA complexes are close packed, but their interlayer distances are somewhat different, suggesting a different tilt of the hydrocarbon chains with respect to the layer plane. The difference in the molecular packing in the room-temperature solid phase of CTAB:BA and CTAB:SA complexes may be partially explained by the closeness of the lengths of CTAB (2.87 nm) and BA (3.0 nm) molecules, while the length of the SA molecule is rather smaller (2.5 nm).

3.2. DSC measurements

DSC curves of CTAB:SA and CTAB:BA complexes measured in a heating run are shown in Fig. 2. Our DSC results are similar to those reported in [9–11] for other long-chain cationics. The prepared compounds demonstrate a complicated thermal behavior with a number of successive phase transitions in the solid state, and the phase behavior of the CTAB:FA complexes is quite different from both of their constituting FA and CTAB components, as follows from the data below.

The phase transition parameters, namely the temperatures and changes in the enthalpy calculated from DSC curves of the investigated complexes, are summarized in Table 1. Table 2 represents the phase transition parameters obtained for the initial compounds SA, BA, and CTAB.

The analysis of DSC data presented in Tables 1 and 2 shows that the thermotropic behavior of the both

complexes is completely different from that of initial components. Contrary to the initial FA with one sharp endothermic transition at the melting point, the both CTAB:FA complexes demonstrate four successive endothermic transitions seen in DSC curves under the heating run in the temperature interval 20–130 °C. The corresponding heat flow peaks do not coincide with the transition points observed for the constituting components. Only for CTAB:BA complex, a small peak is observed at a temperature close to the BA melting temperature, while no peaks close to the SA melting temperature are observed for CTAB:SA. It should be noted that both CTAB:FA complexes show a sharp endothermic peak at nearly the same temperature, which is close to the solid-solid phase transition temperature of CTAB ($T \approx 110$ °C) [15]. Our optical observations show that the melting points of CTAB:SA and CTAB:BA complexes are 110 °C and 107 °C, correspondingly. These points nicely meet the temperature of the main endothermic peak in pure CTAB, although crystalline CTAB does not melt at this temperature. As follows from Tables 1 and 2 for CTAB:FA complexes, ΔH values derived from DSC heating scans for small endothermic peaks observed at the temperatures near the phase transition temperatures of corresponding FA, make up only 10% of their values in the pure FA. At the same time, ΔH value of the main endothermic peak near $T \approx 107$ °C for the both complexes is of the same order of magnitude as that of CTAB. It should be noted that the obtained CTAB:FA compounds undergo melting at a much higher temperature than either of the pure acids. This is a clear indication of the strong interaction between the components and suggests that the investigated materials are not the simple binary mixtures of CTAB and FA, but represent a new supramolecular complex.

The molecular structure of the CTAB:FA complex and the nature of the observed successive thermotropic phase transitions were investigated by FTIR spectroscopy. Temperature-induced changes in the molecular packing and the alkyl chain conformation in the solid phases of the complexes were defined after the detailed study of the spectral parameters of characteristic IR absorption bands.

3.3. FTIR spectroscopy

To characterize the conformational order of the hydrocarbon chains and the head-group structure in

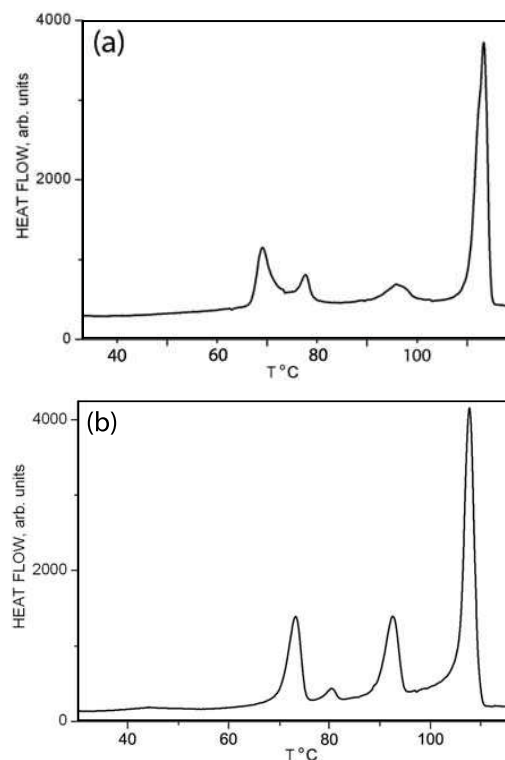


Fig. 2. DSC thermograms for CTAB:SA (a) and CTAB:BA (b) powders in a heating run

Table 1. Phase transition temperatures, T , and enthalpy changes, ΔH , of phase transitions in CTAB:SA and CTAB:BA complexes

Transition No.	CTAB:SA		CTAB:BA	
	T , °C	ΔH , kJ/g	T , °C	ΔH , kJ/g
1	66.0	20	72.9	30
2	74.6	5.4	80.0	2.1
3	92.7	7.3	92.1	22.4
4	110.2	93.6	107.0	72.5

the CTAB:FA complexes at room temperature, we measured FTIR absorption spectra of the complexes and compared them with those of initial FA and CTAB. As an example, FTIR absorption spectra of CTAB:SA complex are shown in Fig. 3 together with those of its pure components – SA and CTAB. Similar spectral patterns are observed for CTAB:BA complex (not shown here). The assignment of the IR spectra of FA and CTAB is well-established, and the

Table 2. Phase transition temperatures, T , and enthalpy changes, ΔH , of phase transitions in polycrystalline SA, BA, and CTAB

Transition No.	$C_{17}H_{35}COOH$ (SA)		$C_{21}H_{43}COOH$ (BA)		CTAB	
	T , °C	ΔH , kJ/g	T , °C	ΔH , kJ/g	T , °C	ΔH , kJ/g
1	–	–	–	–	75.0	1.6
2	70.9	220	80.8	240	106	160.9

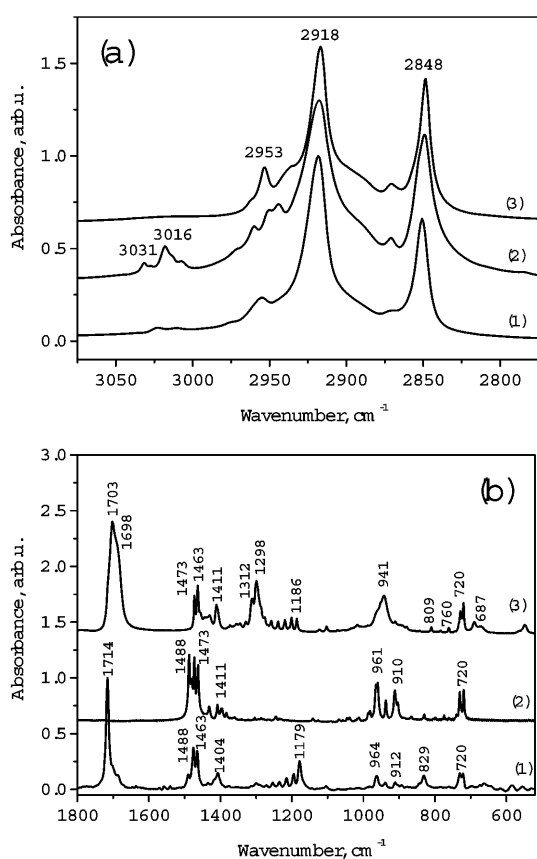


Fig. 3. Room-temperature FTIR absorption spectra of CTAB:SA complex (1) and initial compounds CTAB (2) and SA (3) in the regions of CH stretching (a) and the head-group vibrations (b)

main observed bands, their frequencies and assignments for the investigated compounds could be found, e.g., in [15–19].

It is a common practice to analyze the IR spectra separately by two spectral regions: the high-frequency region containing the absorption bands assigned to CH and OH stretching vibrations (2700–

3100 cm^{-1} , Fig. 3, a), and the low-frequency “fingerprint” region where the bands characteristic of the head-group vibrations (1700–1000 cm^{-1} , Fig. 3, b) could be found. As seen from Fig. 3, a, in the FTIR absorption spectra of CTAB:SA complex in the C–H stretching region between 2800 and 3000 cm^{-1} , the strongest bands located respectively at 2919 cm^{-1} and 2848 cm^{-1} are assigned to alkyl chain asymmetric and symmetric methylene stretching vibrations $\nu_a(CH_2)$ and $\nu_s(CH_2)$, respectively. The weaker bands centered at 3031 and 3016 cm^{-1} originate from CH_3 stretching vibrations of the CTAB residual. The position of CH_2 stretching symmetric and asymmetric vibrations could provide information about the degree of conformational disorder in the methylene chain structure [19–21]. It is known that conformationally ordered state is characterized by a symmetric CH_2 stretching mode frequency below ≈ 2850 cm^{-1} , while the conformational disorder results in a rising of this frequency by several wavenumbers. According to the observed $\nu_a(CH_2)$ and $\nu_s(CH_2)$ bands positions, our FTIR spectra prove a fairly perfect order of the hydrocarbon chains in CTAB:FA complexes with the all-*trans* conformation. In the spectra of pure SA, the broad band with two submaxima extending from ≈ 3200 cm^{-1} to ≈ 2400 cm^{-1} is characteristic of OH stretching vibrations in hydrogen-bonded SA dimers. As is seen from Fig. 3, a, this band is not observed in the FTIR spectrum of CTAB:SA, indicating that the SA-related tails of the complex are in a monomer state.

In “fingerprint” spectral region (below 1700 cm^{-1}) of the FTIR spectra (Fig. 3, b), the band progressions of methylene rocking (700–740 cm^{-1}) and wagging (1180–1410 cm^{-1}) vibrations can be seen, which are characteristic of all-*trans* alkyl chain vibrations. This is another confirmation of the perfect ordering of hydrocarbon chains in CTAB:SA complex. In ad-

dition, in the FTIR spectra of CTAB:SA, a splitting is observed for the methylene scissoring mode (with two components centered at 1472 cm^{-1} and 1463 cm^{-1}) and the methylene rocking mode (with two components at 720 cm^{-1} and 730 cm^{-1}). It is known that the splitting of molecular absorption bands into several components with different polarizations (known as the factor-group or Davydov splitting) appears due to an ordered crystalline environment and is generally observed for crystals with several molecules per unit cell. As was shown in our previous papers [16–18, 22] the appearance of the Davydov splitting in the IR spectra of some solid-phase long-chain aliphatic compounds is related to the fact that their methylene chains packing can be described by an orthorhombic crystal subcell. This unit cell contains two translationally non-equivalent chain fragments, each containing two methylene groups ($-\text{CH}_2-$). The dipole moments corresponding to their vibrations are mutually perpendicular, being parallel to the crystal cell axes, \mathbf{a}_s and \mathbf{b}_s . In this study, the above-mentioned observation of the Davydov splitting suggests an orthorhombic packing of methylene chains in solid-phase CTAB:FA complexes. The temperature dependence of the Davydov splitting value was proven to be a powerful tool for a study of the lattice dynamics and phase transitions in molecular crystals, and the appropriate results will be discussed below in Section 3.4.

Concerning the head-group structure of the complex, the most informative are the IR bands originating from carbon-oxygen vibrations that are observed in the $1500\text{--}1800\text{ cm}^{-1}$ region. The $\nu(\text{C}=\text{O})$ stretching vibration band is highly characteristic of FAs. For a long-chain FA, it is usually observed in the $1690\text{--}1740\text{ cm}^{-1}$ interval. In the FTIR spectrum of pure SA, the carbonyl band is observed at 1702 cm^{-1} with a smaller shoulder at 1687 cm^{-1} , thus indicating that the SA molecules are arranged in H-bonded dimers [12, 19, 23]. As is clearly seen from Fig. 3, the $\text{C}=\text{O}$ stretching band of SA dimers disappears after the complex formation, and a new absorption band emerges at a higher frequency of 1714 cm^{-1} . It should be pointed out that all the other absorption bands related to hydrogen-bonded FA dimers, namely $\nu(\text{OH})$ stretching vibrations band seen as three broad peaks centered at 3000 , 2880 , and 2650 cm^{-1} , corresponding $\delta(\text{OH})$ bending vi-

bration band at 1411 cm^{-1} , as well as other vibrational bands of the dimer ring all completely vanish in the CTAB:SA and CTAB:BA spectra. The observed frequency shifts and the disappearance of the vibration bands characteristic of FA dimers prove that a new CTAB:FA complex is formed. It worth mentioning that the disappearance of the carbonyl stretching band is also observed in the case of FA salt formation. But in our study, no sign of the characteristic absorption of the fatty acid salt occurring at $\approx 1560\text{ cm}^{-1}$ [9–11, 19] is observed in the CTAB:FA FTIR spectra, which suggests the salt-free CAS complex formation. At the same time, the bands of CTAB-related $[\text{N}(\text{CH}_3)_3]^+$ head group, namely $\nu(\text{CH}_3)$ stretching vibration bands centered at 3031 and 3016 cm^{-1} , symmetric and asymmetric $\delta(\text{CH}_3\text{-N}^+)$ bending vibration bands of the head $[\text{N}(\text{CH}_3)_3]$ methyl group centered at 1487 and 1431 cm^{-1} , $\delta(\text{CH}_3)$ bending at 1385 cm^{-1} , and $\nu(\text{CN}^+)$ stretching vibrations at 912 and 904 cm^{-1} , are all present in the spectra of CTAB:FA complexes, being only slightly weakened and broadened. The observed change in the position of $\nu(\text{C}=\text{O})$ stretching vibration band in the FTIR spectra of STAB:FA complexes may be explained either by its strong coupling with the $\delta\text{CH}_3\text{-N}^+$ bending vibrations of the CTAB moiety or by the influence of the electrostatic interaction with nearby cations ($(\text{CH}_3)_3\text{N}^+$). The same features are also observed in the FTIR spectra of CTAB:BA.

So, the analysis of the IR spectra of CTAB:SA and CTAB:BA complexes in the regions of characteristic vibrations of functional groups clearly indicates that the mixing of CTAB and FA in an ethanol solution results in the formation of a supramolecular complex. Though the structure of CTAB:FA complexes is not completely clear at the moment, we suggest that the electrostatic interactions between the oppositely charged ion pairs and a specific molecular geometry of the polar functional groups of CTAB and FA molecules are responsible to a large extent for their complexation. In a specific manner, such complexation may alter physical and chemical properties of the host compound and, in particular, change its thermotropic behavior. In the next section, we investigated the nature of thermotropic phase transitions in the solid phase of the CTAB:FA supramolecular complexes, using temperature-variable FTIR spectroscopy.

3.4. FTIR spectroscopic study of the alkyl chain dynamics and thermotropic phase transitions in CTAB:FA complexes

In this section, we used temperature-variable FTIR spectroscopy to monitor the structural changes accompanying thermal phase transitions in CTAB:FA complexes. As was mentioned above, the frequencies of CH₂ asymmetric and symmetric stretching vibrations are sensitive to the conformational order of the alkyl chains. On the other hand, since the widths of the IR absorption bands are determined by the molecular dynamics such as rotations, translations, and collisions, the CH₂ stretching bandwidths are sensitive to the degree of rotational freedom of CH₂ groups. That is why we used these bands as an indicator of order-disorder transitions of alkyl chains in the solid phase of CTAB:FA complexes.

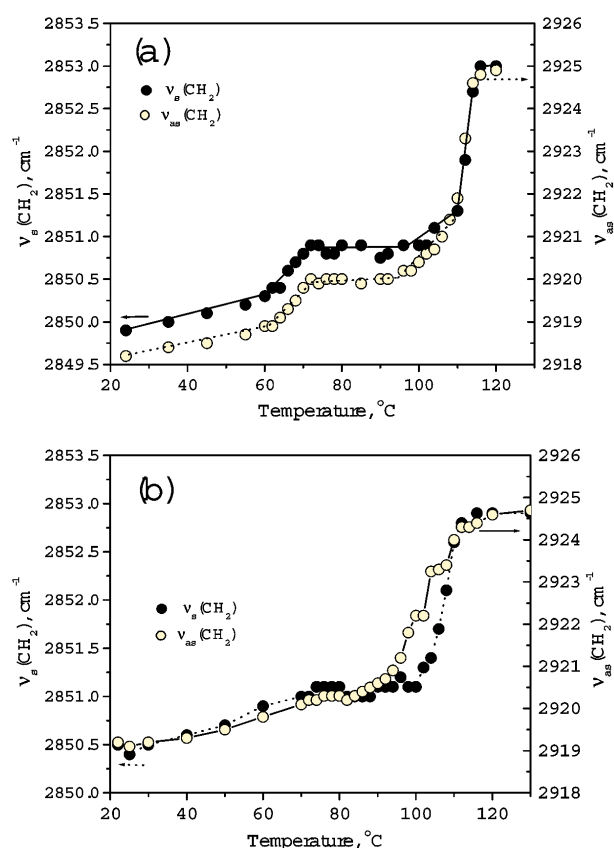


Fig. 4. Temperature dependence of the frequencies of the CH₂ asymmetric, $\nu_a(\text{CH}_2)$ (open circles), and symmetric, $\nu_s(\text{CH}_2)$ (filled circles), stretching bands of CTAB:SA (a) and CTAB:BA (b) complexes

The temperature-dependent changes in the position of the symmetric and asymmetric CH₂ stretching bands (at 2850 cm⁻¹ and 2918 cm⁻¹, respectively) of CTAB:SA and CTAB:BA complexes are shown in Fig. 4.

A shift to higher frequencies with increasing the temperature is clearly seen for the both vibrational bands. The shift occurs smoothly until it reaches some critical point, i.e., the phase transition temperature, where a change of the gradient occurs. As follows from the figure, both CTAB:SA and CTAB:BA complexes have several order-disorder transitions between 60 and 116 °C. The CH₂ stretching frequencies of CTAB:SA complex gradually increase as the temperature increases from 20 to 60 °C, then several changes of the gradient are observed at 60, 74, 95, and 110 °C (Fig. 4, a), indicating the onset of solid-solid phase transitions. The transition points defined from FTIR spectroscopy correlate well with the phase transition temperatures determined by DSC (Table 1). This suggests that, in the temperature interval 60–116 °C, a series of order-disorder transitions in the alkyl chains occurs. A gradual increase of CH₂ stretching frequencies in the temperature range below 110 °C seems to be indicative of the gradual introduction of *gauche* conformers into the alkyl chain over a pre-melting stage. This observation could be proven by small enthalpies of the successive endothermic peaks below the melting point (Table 1), and it probably indicates a partial chain “melting” or pre-transitional chain rotation. This also means that the solid-phase order-disorder transition in CTAB:SA complex occurs over a wider temperature interval than that in pure components. From the comparison of Fig. 4, a and Fig. 4, b, it is obvious that the thermal behavior of the hydrocarbon chains in CTAB:SA is slightly different from that in CTAB:BA. For example, in CTAB:SA, the CH₂ stretching frequencies increase sharply between 110 and 116 °C, whereas they increase slowly in CTAB:BA in a wider temperature interval between 92 and 116 °C, showing a more extended phase transition. The suggested reasons for the different thermal behaviors of the hydrocarbon chains of CTAB:SA and CTAB:BA seem to be as follows. First, it should be noted that the conformational orders of the alkyl chains in the two CTAB:FA complexes are different. The CH₂ stretching frequencies in CTAB:SA are lower than those in CTAB:BA

complex at the same temperature (Fig. 4). At room temperature, the frequency of the CH₂ asymmetric stretching band in CTAB:SA is 2918 cm⁻¹, while it is 2919.5 cm⁻¹ in CTAB:BA. This observation means a higher conformational disorder of alkyl chains in CTAB:BA complex, which correlates well with a larger molecular tilt angle determined by XRD. The differences in the conformational order of the alkyl chains could affect their packing in the solid phases of CTAB:FA complexes. Another reason may come from the different balances of the van der Waals and electrostatic forces in the layered structure of the complexes.

We obtained more information about the nature of the phase transitions in solid CTAB:FA complexes from the analysis of FTIR spectra in the region of the Davydov splitting (DS) of CH₂ rocking vibrations (720–730 cm⁻¹). In our previous papers [16–18, 22], we showed that the temperature variation of the DS value ($\Delta\nu_{1,2}$) of vibrational excitons is helpful to study the lattice dynamics and changes in the molecular packing under phase transitions in molecular crystals. According to the theory [24], the elements of the dynamic matrix for the resonance molecular interaction D that determines the DS value do not depend on the absolute position of atoms in the interacting molecules but only on the distance between them being inversely proportional to r^3 . In the case of orthorhombic unit cell, r is a distance between non-equivalent –CH₂– methylene groups in a unit cell. So, the Davydov splitting value depends on the unit cell parameters of a crystal. It is clear that any distortion in the periodic location of molecules would affect the molecular interactions. In particular, one could expect a variation in the DS value under a transition into an orientationally disordered phase.

Figure 5 shows the DS value and the full width at half maximum (FWHM) for the band of CH₂ rocking vibrations in the FTIR spectra of CTAB:FA complexes and their pure components as a function of the temperature. One can see that the DS value gradually decreases with the temperature for both complexes, the decrease being more rapid for CTAB:BA than that for CTAB:SA or pure acids. Since the DS value is inversely proportional to r^3 , this observation suggests a significant difference in the alkyl chains packing behaviors in CTAB:SA and CTAB:BA at elevated temperatures. The DS value

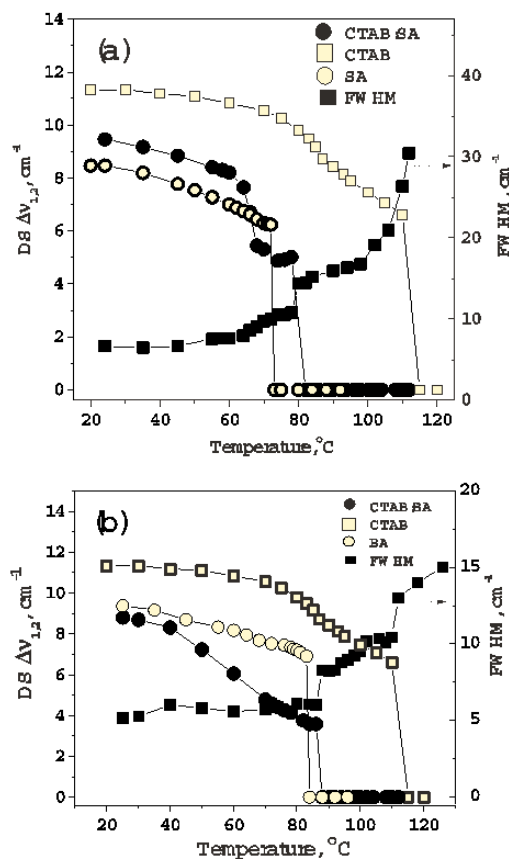


Fig. 5. Temperature dependence of the DS value ($\Delta\nu_{1,2}$) and the band width (FWHM) for CH₂ rocking vibrations in the FTIR spectra of CTAB:SA (a) and CTAB:BA (b) and pure components

drops to zero at 78 and 86 °C for CTAB:SA and CTAB:BA, respectively. In both complexes, a simultaneous sharp increase of FWHM is observed at these points. Since, at these transition temperatures, a conformational disorder of alkyl chains, which is seen from an increase of the CH stretching frequencies (Fig. 4), continues to develop, all these changes are indicative of a solid-solid phase transition accompanying a change in the packing of methylene chains from the orthorhombic into another crystalline phase. A drastic increase of FWHM by about 40% under the phase transition means that, in this new phase, the methylene chains are in a dynamically disordered state or hindered rotation and are packed in the so-called rotator phase [25]. The obtained phase transition temperatures are close to the melting points of the correspond-

ing FA, so the observed DS is attributed rather to the resonance molecular interaction of acid-related methylene chains than to CTAB-related ones. The transition point to the rotary phase is higher for CTAB:BA, thus suggesting a higher stability of this complex due to the longer BA alkyl chain length. This means that the molecular interaction between the acid-related alkyl fragments of CTAB:FA complex dominates, and is mainly responsible for structural deformations under the phase transitions. Presumably, the CTAB-related methylene chains penetrate into the structure of the complex in a specific packing which is different from that of pure CTAB starting from room temperature. It worth noting that the CTAB:FA solid-solid phase transition points defined from the temperature variation in DS are close to the first low-enthalpy transition point for corresponding complexes defined from DSC measurements (Table 2). This clearly indicates that the successive low-enthalpy endothermic phase transitions occurring in CTAB:FA complexes are related to a cooperative dynamical disorder in their structure due to hindered molecular rotations of alkyl chains. As we have already mentioned, according to our microscopic observations, CTAB:SA and CTAB:BA complexes do not melt at the fusion point of corresponding acid, the melting temperature of the CTAB:FA complex being about 50 °C higher. This suggests that the incorporation of CTAB molecules with a positively charged bulky head group (comprising three methyl groups) contributes to the electrostatic interactions in the ionic layer, thus significantly improving the thermal stability of the host crystal lattice.

Summarizing, the FTIR spectroscopic study suggests a cooperative thermotropic phase transition process in CTAB:FA complexes that involves the “melting” of alkyl chains over a series of successive solid-solid phase transitions accompanied by a change in the packing of methylene chains from the orthorhombic into so-called rotary crystalline phase, followed by a further disintegration of the ionic layer at the melting point. The complexation of FA molecules with CTAB leads to a greatly enhanced thermotropic stability of the host compound.

4. Conclusions

A simple method was developed to obtain a supramolecular catanionic complex comprising a

cationic CTAB and SA or BA fatty acid tails by the mixing of equimolar ethanol solutions. The X-ray diffraction studies show a layered crystalline structure for both CTAB:SA and CTAB:BA complexes. The DSC study revealed a series of solid-solid phase transitions in CTAB:SA and CTAB:BA complexes at temperatures below the melting point, the latter being close to the temperature of a solid-solid phase transition in CTAB. The greatly enhanced thermal stability of the CTAB:FA complexes as compared with that of the pure acids (by ≈ 50 °C) is shown. The FTIR spectroscopic results suggest a cooperative thermotropic phase transition process in CTAB:FA complexes that involves the “melting” of alkyl chains over a series of successive solid-solid phase transitions accompanied by a change in the packing of methylene chains. Our research provides a molecular basis for the prospective application of such class of complexes in thermo-sensitive supramolecular systems.

The authors are deeply thankful to Prof. V.G. Il'jin for the help with X-ray diffraction measurements. We gratefully appreciate the financial support from the National Academy of Science of Ukraine under “Nanophysics and Nanoelectronics” program (project No. VC-157).

1. D. Kopetzki, Y. Michina, T. Gustavsson, and D. Carriere, *Soft Matter* **5**, 4212 (2009).
2. Th. Zemb, D. Carriere, K. Glinel, M. Hartman, A. Meister, Cl. Vautrin, N. Delorme, A. Fery, and M. Dubois, *Colloid Surface A* **303**, 37 (2007).
3. A. Stocco, D. Carriere, M. Cottat, and D. Langevin, *Langmuir* **26**, 10663 (2010).
4. M. Dubois, D. Carriere, R. Iyer, M. Arunagirinathan, J. Bellare, J. Verbavatz, and T. Zemb, *Colloid Surface A* **319**, 90 (2008).
5. E. Maurer, L. Belloni, T. Zemb, and D. Carriere, *Langmuir* **23**, 6554 (2007).
6. G. Andreatta, J.-J. Benattara, R. Petkova, J.Y.J. Wang, P. Tong, A. Polidori, and B. Pucci, *Colloid Surface A* **321**, 211 (2008).
7. Y. Lu, R. Gangull, C. Drewlen, M. Anderson, C. Brinker, W. Gong, Y. Guo, H. Soyez, B. Dunn, M. Huang, and J. Zink, *Nature* **389**, 364 (1997).
8. S. Biswas, S.A. Hussain, S. Deb, R.K. Nath, and D. Bhattacharjee, *Spectrochim. Acta A* **65**, 628 (2006).
9. V. Tomasić, S. Popović, and N. Filipovic-Vinceković, *J. Colloid Interf. Sci.* **215**, 280 (1999).

10. M.L. Lynch, F. Wireko, M. Tarek, and M. Klein, *J. Phys. Chem. B* **105**, 552 (2001).
11. N. Filipovic-Vinceković, I. Pucić, S. Popović, V. Tomasić, and D. Tezak, *J. Colloid Interf. Sci.* **188**, 396 (1997).
12. J.B. Peng, G.T. Barnes, and I.R. Gentle, *Adv. Colloid Interf. Sci.* **91**, 163 (2001).
13. B.F.B. Silva, E.F. Marques, U. Olsson, and R. Pons, *Langmuir* **26**, 3058 (2010).
14. B. Tah, P. Pal, M. Mahato, and G.B. Talapatra, *J. Phys. Chem. B* **115**, 8493 (2011).
15. T. Bezrodna, G. Puchkovska, V. Styopkin, and J. Baran, *Thin Solid Films* **517**, 1759 (2009).
16. T. Bezrodna, G. Puchkovska, V. Styopkin, J. Baran, M. Drozd, V. Danchuk, and A. Kravchuk, *J. Molec. Struct.* **973**, 47 (2010).
17. S.P. Makarenko, G.A. Puchkovska, E.N. Kotelnikova, and S.K. Filatov, *J. Molec. Struct.* **704**, 25 (2004).
18. G.O. Puchkovska, S.P. Makarenko, V.D. Danchuk, and A.P. Kravchuk, *J. Molec. Struct.* **744–747**, 53 (2005).
19. L.J. Bellami, *The Infra-Red Spectra of Complex Molecules* (Wiley, New York, 1958).
20. W. Wu, Y. Wang, and H.-S. Wang, *Vib. Spectrosc.* **46**, 158 (2008).
21. A. Imanishi, R. Omoda, and Y. Nakato, *Langmuir* **22**, 1706 (2006).
22. G.O. Puchkovska, V.D. Danchuk, A.P. Kravchuk, and J.I. Kukielski, *J. Molec. Struct.* **704**, 119 (2004).
23. D. Hadži, J. Grdadolnik, and A. Meden, *J. Molec. Struct.* **381**, 9 (1996).
24. A.S. Davydov, *Theory of Molecular Excitons* (Plenum Press, New York, 1971).
25. E.B. Sirota, H.E. King, jr., D.M. Singer, and H.S. Shao, *J. Chem. Phys.* **98**, 5809 (1993).

Received 18.04.13

Т.А. Гаврилко, Г.О. Пучковська, В.І. Стъопкін,
Т.В. Безродна, Я. Баран, М. Дрозд

МОЛЕКУЛЯРНА
ДИНАМІКА ТА ФАЗОВІ ПЕРЕТВОРЕННЯ
У БІНАРНИХ СУМІШАХ ЖИРНИХ КИСЛОТ
ТА ГЕКСАДЕЦИЛТРИМЕТІЛАМОНІУМБРОМІДУ:
ДОСЛІДЖЕННЯ ДАВИДОВСЬКОГО РОЗЩЕПЛЕННЯ
МОЛЕКУЛЯРНИХ КОЛИВАЛЬНИХ МОД

Резюме

Досліджено твердофазні 1:1 комплекси, що складаються зі стеаринової або бегенової кислоти (СА або ВА відповідно) та гексадецилтриметіламоніумбромиду (СТАВ) – катіонної поверхнево-активної речовини, отримані з відповідних еквімолярних розчинів в етанолі. Утворення супрамолекулярного комплексу між молекулами жирних кислот та СТАВ підтверджують дані ІЧ-спектроскопії, дифракції рентгенівських променів та диференційної сканувальної калориметрії (ДСК). Дані рентгенівської дифракції свідчать про утворення шаруватої кристалічної структури для обох досліджених комплексів – СТАВ:СА і СТАВ:ВА. За допомогою методу ДСК виявлено значне підвищення термічної стабільності утворених комплексів порівняно з чистими кислотами (підвищення температури плавлення приблизно на 40–50 °С) та існування кількох послідовних фазових переходів. Досліджено температурну залежність величини давидовського розщеплення в ІЧ-спектрах досліджених комплексів для коливальних смуг маятникових коливань метиленових груп (спектральна ділянка 720–730 см⁻¹). Виявлено значні відмінності у конформації метиленових ланцюжків та упакуванні молекул у послідовних фазових станах двох комплексів залежно від довжини алкільного ланцюга кислотного фрагмента. Отримані результати можуть правити за основу для подальшого застосування досліджуваних бінарних сумішей катіонних та аніонних ПАВ при розробці термочутливих супрамолекулярних систем.